Water-Body Area Extraction from High Resolution Satellite Images-An Introduction, Review, and Comparison

Rajiv Kumar Nath   rajivknath@gmail.com
Research Scholar, Department of Civil Engineering
IIT Delhi
New Delhi, 110016, India

S K Deb   skdeb@hotmail.com
Assistant Professor, Department of Civil Engineering
IIT Delhi
New Delhi, 110016, India

Abstract

Water resources play an important role in environmental, transportation and region planning, natural disaster, industrial and agricultural production and so on. Surveying of water-bodies and delineate its features properly is very first step for any planning, especially for places like India, where the land-cover is dominated by water-bodies. Recording images, such as from satellite, sometimes does not reflect the distinguished characteristics of water with non-water features, e.g. shadows of super structures. Image of water body is confused easily with the shadow of skyscraper, since calm water surface induces mirror reflection when it gives birth to echo wave. Water transport is cheapest. Developing/poor countries like India will be benifitted if water transport is encouraged. In water transport, the link should be made between various land masses, including building blocks, through proper navigational system. Hence there should be clear distinction between calm water and the shadows of buildings. Over the past decade, a significant amount of research been conducted to extract the water body information from various multi-resolution satellite images. The objective of this paper is to review methodologies applied for water body extraction using satellite remote sensing. The Geographic Information System (GIS) and the Global Positioning System (GPS) have also been discussed as they are closely linked with Remote Sensing. Initially, studies on water body detection are treated. Methodological issues related to the use of these methods were analysed followed by summaries. Results from empirical studies, applying water-body extraction techniques are collected and discussed. Important issues for future research are also identified and discussed.

Keywords: Feature extraction, multi-resolution satellite image, remote sensing, and water body.

1. INTRODUCTION

Watershed is a region (or area) delineated with a well-defined topographic boundary and water outlet. It is a geographic region within which hydrological conditions are such that water becomes concentrated within a particular location, for example, ocean, sea Lake, a river, or a reservoir, by which the watershed is drained. Within the topographic boundary or a water divide, watershed comprises a complex of soils, landforms, vegetations, landform and land uses. The terms watershed, catchment, and basins are often considered synonyms [1]. Remote sensing, defined as the science of using an instrument for measuring a target and its properties from a remote location, without a physical connection between the measuring instrument and the target, which is to be featured. Typically, the measurements are performed through various techniques. Those techniques are electromagnetic radiation (e.g. ultra-violet, visible light, reflective, thermal infrared, microwaves, etc.). The instrument records the radiation reflected or emitted by the target and its properties are then inferred from the measured signal.

One of the advantages of remote sensing is that the measurements can be performed from a great distance (several hundred or even several thousand kilometers in the case of satellite sensors), which means that large areas on ground can be covered easily. With satellite instruments it is also possible to observe, a target repeatedly; in some cases every day or even several times per day.

Classification is a widely studied issue in remote sensing image processing. The common application ranges from land use analysis to change detection. Among the classes of interest, urban areas, farmland, forest, and river/lake areas are traditionally selected. The observation of water body from remote sensing images, is of particular importance during these recent years for two main reasons: (i) there is a world-wide an important need to assess existing water resource and water resource changes –because of the increasing water scarcity and related problems; (ii) the so-called "climate change" affects directly and is directly affected by water cycling; (iii) study of water bodies may help to develop water transport route, either by using existing one directly or connecting the existing one by preparing canals to develop a longer water route; (iv) timely information of water increase in hills and mountains may help to develop some strategy to restrict flood calamities. Remote sensing and its allied techniques such as geographic information system have a pervasive impact on the conduct of practical work. The application of these are in business, ecology, engineering, forestry, geography, geology, urban and regional planning, water resources management, transportation engineering or environmental science Remote sensing data provides a mean to observe and analyze some of the related phenomena, such as flood disasters and land use change. There exist a close interaction among the related areas of remote sensing, GIS, GPS, digital image processing and environmental, transportation and regional medelling.

The ability to map open surface water is an integral part to many hydrologic and agricultural models, wildlife management programmes, and recreational and natural resource studies. The study of X-band *HH* polarized airborne Synthetic Aperture Radar (SAR) imagery to examine the potential of SAR data to map open fresh water areas extant on 1:100000 USGS topographic maps [2] and SAR image based on technique of imaging in different directions and object-oriented [3]. The remote sensing- GIS techniques used for identification of various land-use classes on satellite imagery and enhanced products and identification of time-sequential changes in land-use patterns [4]. A new model based on EOS/MOSDIS model which can segment the water body and extract by the criteria of NDWI<-0.1 or NDVI<0.04 & (CH4-CH5)>2.0 [5]. The decision tree and programming method is used for extracting water body information from flood affected region [6],[7]; semi-automated change detection approach is used for extracting water feature form satellite image [8],[9],[10],[11]; an automatic extraction method is used for extracting water body from IKONOS and other high resolution satellite image [12],[13],[14]; Thresholding and multivariate regression method [15], A conceptual clustering technique and dynamic Thresholding [16], an original entropy based method [17]. The water body can be extracted by

classification; unsupervised classification [18]; The Euclidean Classifier and the Eigenvector Classifier [19]; The SVM with One-Against-One (1A1) and One-Against-All (1AA) techniques is used for land cover mapping [20] ; A supervised classification algorithm [21],[22] of remote sensing satellite image that uses the average fuzzy intra cluster distance within the Bayesian algorithm [23],[24]; sometimes combination of supervised and unsupervised classification is used also called automated [25], The edge detection algorithm [26], the data fusion technique is used to characterize and delineate 1993 flood damage in the Midwest of St. Luis, USA [27]; a remote sensing and Geographical Information System (GIS) to estimate and hindcast water quality changes using historical land use data for a watershed in eastern England [28],[29]. Some researches focused on the water quality of the specific water body, in this; first, we extract the water body then assess the water quality [30], [31], [32].

2. SATELLITES AND SENSORS APPLIED IN WATER BODY EXTRACTION

A large number of earth observation satellites has orbited, and is orbiting our planet to provide frequent imagery of its surface. From these satellites, many can potentially provide useful information for assessing erosion, although less has actually been used for this purpose. This section provides a brief overview of the space borne sensors applied in water-body extraction studies. The sensors can be divided in those measuring reflection of sunlight in the visible and infrared part of the electromagnetic spectrum and thermal infrared radiance (optical systems), and those actively transmitting microwave pulses and recording the received signal (imaging radars).

Optical satellite systems are most frequently been applied in water body extraction research. The parts of the electromagnetic spectrum covered by these sensors include the visible and near-infrared (VNIR) ranging from 0.4 to 1.3 μm, the shortwave infrared (SWIR) between 1.3 and 3.0 μm, the thermal infrared (TIR) from 3.0 to 15.0 μm and the long-wavelength infrared (LWIR) from (7-14 µm). Table 1 summarizes sensor characteristics of the systems used [33], [34], [35].

Satellite	Sensors	Operation Time	Spatial resolution	# spectral bands	Spectral domain
Landsat-1,2,3	MSS	1972-1983	80m	4	VNIR
NOAA/ TIROS	AVHRR	1978-present	1001m	5	VNIR, SWIR, TIR
Nimbus-7	CZCS	1978-1986	825m	6	VNIR
Landsat-4,5	TM	1982-1999	30m 120m	6 1	VNIR, SWIR TIR
SPOT-1,2,3	HRV	1986-present	10m 20m	1 3	VNIR VNIR
IRS-1A,1B	LISS-1 LISS-2	1988--1999	72.5m 36.25m	4 4	VNIR VNIR
IRS-1C,1D	PAN LISS-3	1995-present	5.8m 23.5m 70m	1 3 1	VNIR VNIR SWIR
SPOT-4	HRVIR	1998-present	10m 20m	1 4	VIS VNIR, SWIR
IKONOS	Panchromatic Multispectral	1999-present	1m 4m	1 4	VNIR VNIR
Landsat-7	ETM	1999-present	15m 30m 60m	1 6 1	VNIR VNIR TIR
Terra	ASTER MODIS	1999-present 1999-present	15m 30m 90m 250m 500m 1000m	3 6 5 2 5 29	VNIR SWIR TIR VIS NIR SWIR/ MWIR LWIR
Quick Bird	Panchromatic Multispectral	2001-present	0.61m 4m	1 4	VNIR VNIR
SPOT-5	Panchromatic Multispectral	2002- present	5m 10 10m 20m	1 4	VNIR NIR SWIR
WorldView-1	Panchromatic	2007-present	0.55m	1	VIR NIR
GEOEYE-1	Pan-sharpened Panchromatic Multispectral	2008-present	0.41m 0.41m 1.65m	3 1 4	VIR NIR

TAB
LE 1: Overview of optical satellite sensors applied in water body extraction

Landsat is still among the widest used satellites, partly because it has the longest time series of data of currently available satellites. The first satellites of the Landsat family were equipped with the Multispectral Scanner (MSS), having four bands at 80-m resolution. AVHRR (Advanced Very

High Resolution Radiometer) has five bands in 1.1-km resolution and has been flown on many platforms, including TIROS-N (Television Infrared Observation System) and several NOAA-satellites (National Oceanic and Atmospheric Administration).

Later Landsat satellites had the Thematic Mapper (TM) sensors onboard with improved resolution and more spectral bands. The SPOT series of satellites started acquiring data in 1986 with the HRV-sensor (High Resolution Visible). The HRV-sensor has a 10-m panchromatic mode and a three band 20-m resolution multispectral mode. The Indian Remote Sensing Satellites (IRS) 1A and 1B both have two sensors called LISS-1 and LISS-2 (Linear Imaging and Self-Scanning Sensor), which are identical except for a two times higher spatial resolution on LISS-2. IRS 1C and 1D also have an identical payload being a 5.8-m resolution panchromatic camera (PAN) and a 23.5-m resolution multispectral sensor called LISS-3. SPOT-4 flew the HRVIR-sensor (High Resolution Visible Infrared) on which a SWIR band was added. IKONOS and QuickBird are both high-resolution satellites, with a spatial resolution in panchromatic mode of 0.61 and 1.00 m respectively, and 2.44 and 4.00 m in multispectral mode. The start of space borne imaging radar instruments was in 1978 with the SAR (synthetic aperture radar) onboard SEASAT, operating in L-band (23.5-cm wavelength) during 105 days only. For erosion studies, only five SAR sensors have been applied, which were flown on ERS-1 and 2, JERS-1, RADARSAT-1, and ENVISAT respectively. In 1991, ERS-1 launched with the Active Microwave Instrument (AMI) onboard operating in C-band (5.7-cm wavelength). The SAR image mode of AMI acquired data at 30-m resolution. ERS-2 flies the same instrument and has been operational from 1995 to till present. JERS-1 (Japanese Earth Resources Satellite) flew an 18-m resolution L-band SAR (23.5-cm wavelength), recording data from 1992 to 1998. RADARSAT-1 has acquired C-band SAR data since 1995 and has the possibility of using a variety of incidence angles (between 20° and 49°) and different resolutions (between 10 and 100 m). The Advanced SAR (ASAR) onboard ENVISAT, launched in 2002, also has the possibility of using several incidence angles (between 15° and 45°). Besides, the C-band SAR can transmit and receive radar pulses both in horizontal and vertical polarization, which refers to the plane in which the electromagnetic wave is propagating. Spatial resolutions of ASAR are approximately 30 m, 150 m, or 1 km, depending on the mode used. Landsat satellites had the enhanced TM (ETM) sensors onboard with improved resolution and more spectral bands. ASTER (Advanced Space borne Thermal Emission and Reflection Radiometer) is one of the sensors onboard the Terra satellite. It has 14 spectral bands of which several are situated in the SWIR and TIR regions. One near infrared (NIR) band looks both nadir and backward creating stereo-view from a single pass. MODIS (Moderate Resolution Imaging Spectroradiometer) is one of the sensor onboard the Terra (EOS AM) and Aqua (EOS PM) satellites. It has five bands near infrared. It has 29 bands of which several are situated in the SWIR/MWIR and LWIR regions.

3.0 OVERVIEW OF EXISTING METHODS
3.1 Feature extraction method
1) The Entropy Based Water Body extraction method has been tested on ERS SAR amplitude data, SPOT HRV, and LANDSAT-7 ETM+ panchromatic images. Figure 1, shows the water areas extraction in Hubei Province of China about LANDSAT-7 ETM+ image and Figure 2 shows an example of extraction process from ERS SAR amplitude image on Poyang Lake of China. Because of the speckle effect in SAR images, the method works better for optical images than that for SAR images. The details of the water area border smoothed slightly in the course of post-processing.
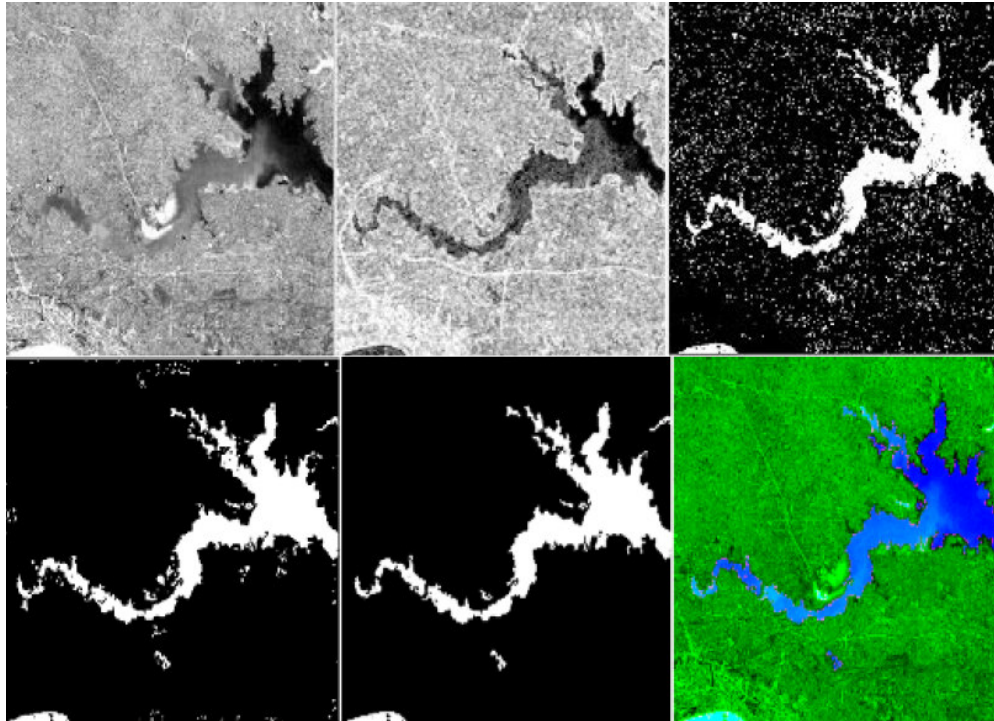
Figure 1: LANDSAT-7 ETM+ image (1000 by 1000 pixels). From left to right: (a) Input image, (b) Entropy data from step 2, (c) Segmented result From step 3, d) Post-processing in step 4, (e) Extracted Water body, and (f) Overlaid with the input image.
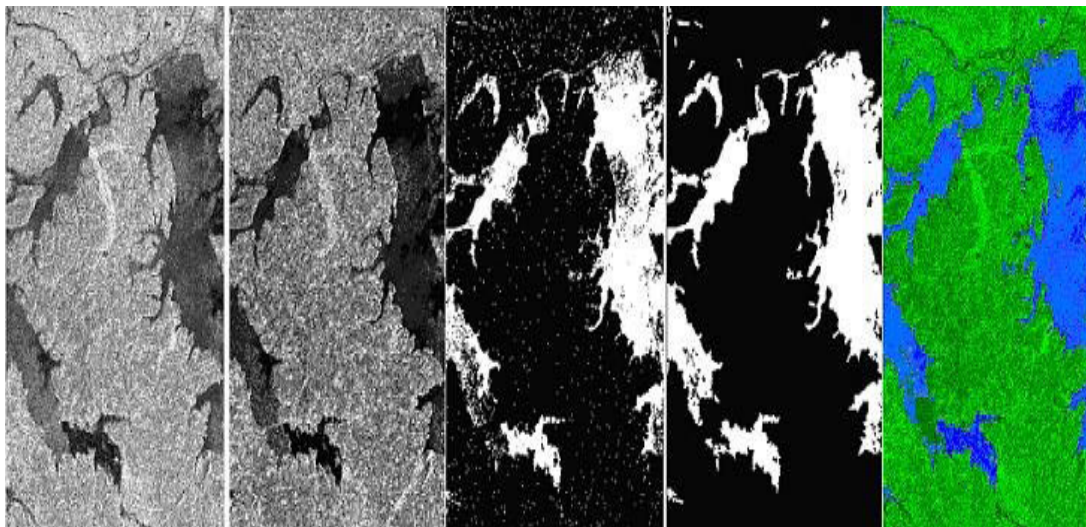

Figure 2: ERS SAR PRI image about Poyang Lake, China (1800 by 3000 pixels) From left to right: (a) Input Image, (b) Entropy Image, (c) Segmented results, (d) After post-processing, and (e) Overlaid with the input image

2) In general, images have the following features – color, texture, shape, edge, shadows, temporal details etc. The most promising features were color, texture, and edge. These features are extracted individually from the satellite and combined to get the final extracted image.

3) The mean shift algorithm is a powerful technique for image segmentation. The algorithm recursively moves to the kernel smoothed centroid for every data point. The quadratic computational complexity of the algorithm is a significant barrier to the scalability of this algorithm

to practical applications. The fast Gauss transform (FGT) has successfully accelerated the kernel density estimation to linear running time for low-dimensional problems. Unfortunately, the cost of a direct extension of the FGT to higher-dimensional problems grows exponentially with dimension, making it impractical for dimensions above three [36], [37]. An image segmented into homogeneous regions by mean shift segmentation. Then, the major water body, identified and an initial shoreline generated. The final shoreline obtained by local refinement within the boundaries of the candidate regions adjacent to the initial shoreline.

4) Skeletonization is the process of peeling off of a pattern as many pixels as possible without affecting the general shape of the pattern [38], [39]. In other words, after pixels have been peeled off, the pattern should still be recognized. The skeleton hence obtained must have the following properties: 1) as thin as possible; 2) connected; and 3) centered. The water-body feature extracted from satellite imagery with a combination of two processes. This process includes the boundary extraction and skeletonization from color imagery using a color image segmentation algorithm, a crust extraction algorithm, and new skeleton extraction algorithm.
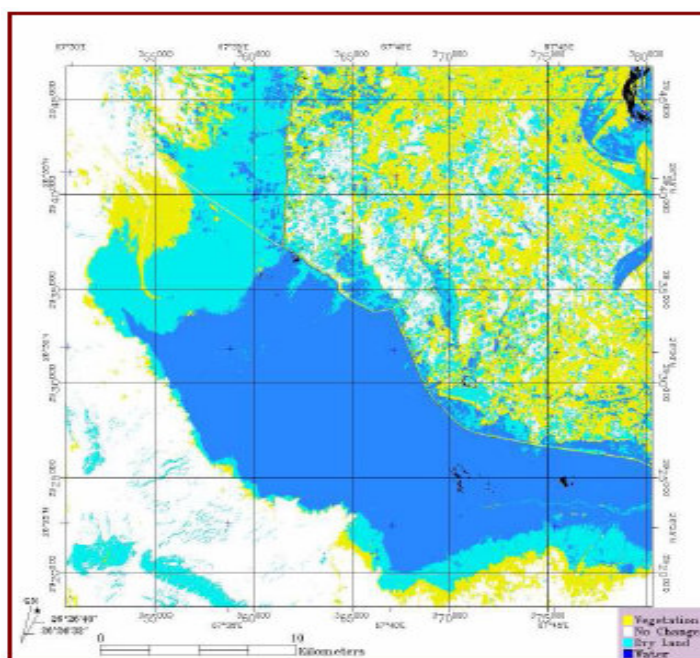

Figure 3: Result of Change detection 1992/2003

3.2 Supervised and Unsupervised Classification method

Advances in sensor technology for Earth observation make it possible to collect multispectral data in much higher dimensionality. In addition, multisource data also will provide high dimensional data. Such high dimensional data will have several impacts on processing technology: (1) it will be possible to classify more classes; (2) more processing power will be needed to process such high dimensional data (3) with large increases in dimensionality and the number of classes, processing time will increase significantly.

The analysis of remotely sensed data is usually done by machine oriented pattern recognition techniques. One of the most widely used pattern recognition techniques is classification based on maximum likelihood (ML) assuming Gaussian distributions of classes. A problem of Gaussian ML classification takes long processing time. The long processing time leads to long computational time and as a result computational cost rises. This computational cost may become an important problem if the remotely sensed data of a large area is to be analyzed or if the processing hardware is more modest in its capabilities. The advent of the future sensors will aggravate this

problem. Hence, attention should be paid to extract detailed information from high dimensional data while reducing processing time considerably [40].

There are various types of supervised classification method are used to classify the water body from high-resolution satellite images.

1) The supervised classification is used to classify the satellite image of years (1992 and 2003) in three different classes namely blue color for water, green for the vegetation and aqua for dry land and these results are compared to find out the change in the Mancher Lake of Pakistan . Report shows that number of points (Npts) selected for the sample region on the image and percentage (Pct) show the area of water, vegetation, and dry land that is shown in table 2 and figure 4.

For 1992

Class Name	Npts	Pct (%)
Unclassified	[0]	0.00
Vegetation	[242754]	23.119
Water	[530251]	35.049
Dry Land	[665373]	43.980

For 2003

Class Name	Npts	Pct (%)
Unclassified	[0]	0.00
Vegetation	[317276]	20.971
Water	[202640]	19.299
Dry Land	[604606]	57.582

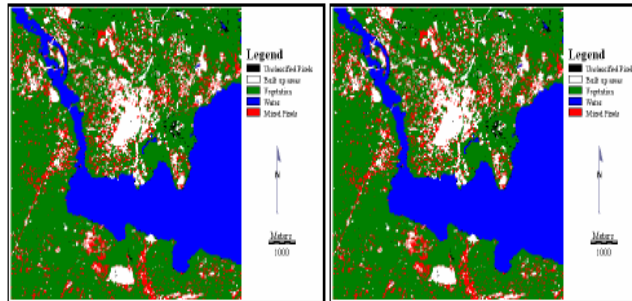**Table 2**: The percentage of water and other classified data

Figure 4a 1A1 Linear   **Figure 4b** 1AA Linear

2) Support Vector Machine with One-Against-One (1A1) and One-Against-All (1AA) techniques is used for land cover mapping of the Landsat Scene located at the source of River Nile in Jinja, Uganda. The bands used in this research consisted of Landsat's optical bands i.e. bands 1, 2, 3, 4, 5, and 7. The classes of interest were built up area, vegetation, and water. Table 3 gives a summary of the unclassified and mixed pixels resulting from 1A1 and 1AA classification. From Table 3 it is evident that the 1AA approach to multiclass classification has exhibited a higher propensity for unclassified and mixed pixels than the 1A1 approach. From Table 4, all accuracies would be classified as yielding very strong correlation with ground truth data. The individual performance of the SVM classifiers however show that classification accuracy reduced for the linear and RBF classifiers stayed the same for the polynomial and increased for the quadratic classifier.

Classifier	Type	1A1	1AA
Linear	Unclassified Pixels	16	700
	Mixed Pixels	0	9048
Quadratic	Unclassified Pixels	142	5952
	Mixed Pixels	0	537
Polynomial	Unclassified Pixels	69	336
	Mixed Pixels	0	2172
RBF	Unclassified Pixels	103	4645
	Mixed Pixels	0	0

TABLE 3: Summary of number of unclassified and mixed pixels

Further, analysis of these results shows that these differences are pretty much insignificant at the 95% confidence interval. It can therefore be concluded that whereas one can be certain of high classification results with the 1A1 approach, the 1AA yields approximately as good classification accuracies.

SVM	1A1	1AA	|Z|	Significance
Linear	1.00	0.95	0.06	Difference insignificant
Quadratic	0.88	0.94	-0.02	Difference insignificant
Polynomial	1.00	1.00	0.0	No difference
RBF	0.97	0.92	0.01	Difference insignificant

TABLE 4: Summary of number of unclassified and mixed pixels
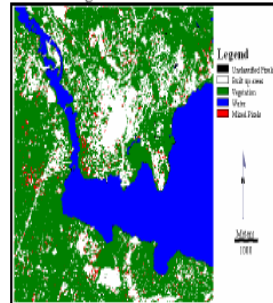

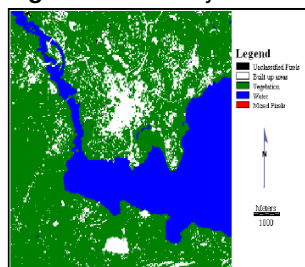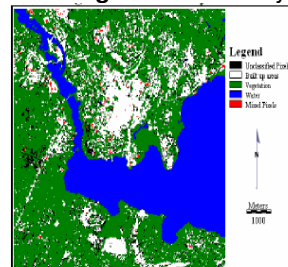**Figure 5a** 1A1 Polynomial   **Figure 5b** 1AA Polynomial

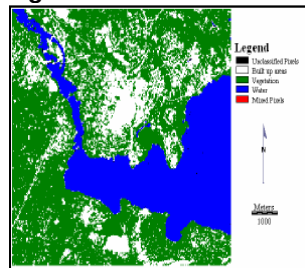**Figure 6a** 1A1 Quadratic   **Figure 6b** 1AA Quadratic

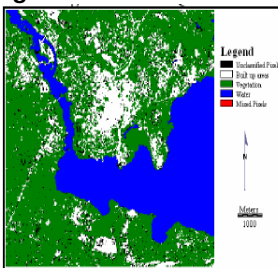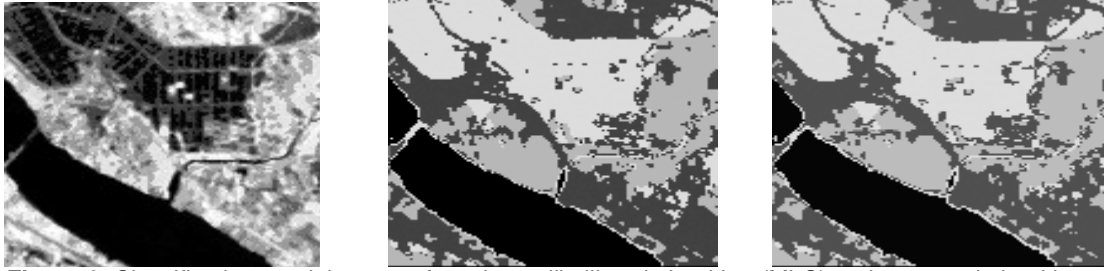**Figure 7a** 1A1 RBF   **Figure 7b** 1AA RBF

Figure 8: Classification result images of maximum likelihood algorithm (MLC) and proposed algorithm using Landsat TM satellite image

The author proposed a Learning Vector Quantization (LVQ) neural network method for automatic extraction of water bodies from Landsat 4 satellite image. In this work, Landsat Thematic Mapper(TM) sensor image of Mississippi river region of 1986 was used. It is a supervised classification method and aims to define the decision surface between competing classes. They compared their results with Tasseled Cap Transformation (TCT) and conventional rule based method. It observed that the result obtained by LVQ method is poor than rule based and TCC methods but the later two methods need human guidance while LVQ method is automatic [41].

3) The Bayesian supervised algorithm using the average intracluster distance within the fuzzy Gustafson-Kessel (GK) and Bayesian algorithm. The suggested algorithm uses the fuzzy GK algorithm in the form extended for the FCM. Different cluster distributions and sizes usually lead to sub optimal results with FCM. In order to adapt to different structures in data, GK algorithm used the covariance matrix to capture ellipsoidal properties of cluster. It makes classification of the remote sensing satellite image with multidimensional data possible. Fuzzy algorithm generally iterates the execution until there is almost no change in membership value.
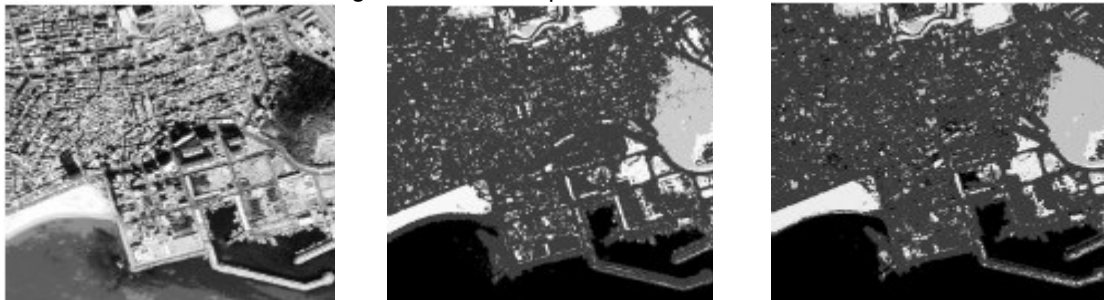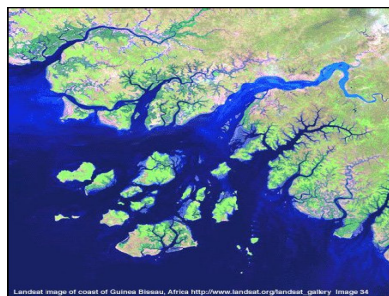

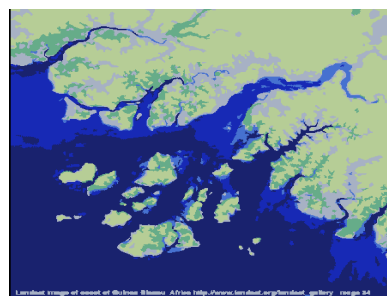a) Original Image   (b) MLC Image   (c) Proposed Algorithm Image

Figure 9: Classification result images of maximum likelihood algorithm (MLC) and proposed algorithm using IKONOS satellite image.

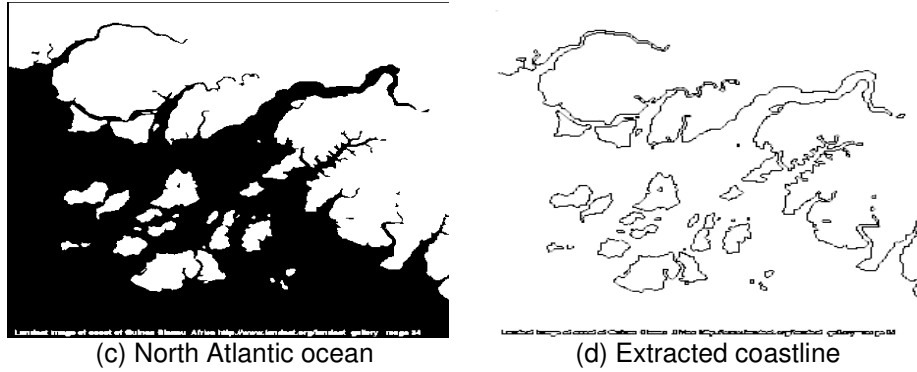(a) Satellite image of Guinea Bissau   (b) Over-segmented image

(c) North Atlantic ocean   (d) Extracted coastline

Figure 10: Feature boundary extraction from the satellite image of Guinea Bissau

Category		Forest	Water	Crop	Urban	Overall accuracy
Number of training pixels		1024	1024	1024	1024	4096
Classification methods	Maximum likelihood	90.43%	98.05%	92.48%	89.06%	92.50%
	FCM	85.15%	97.46%	85.83%	92.45%	90.22%
	Proposed method	91.25%	98.53%	93.45%	92.45%	93.92%

TABLE 5: The classification results by proposed algorithm, conventional maximum likelihood and FCM algorithm from Landsat TM resolution satellite image

Category		Forest	Water	Soil	Urban	Overall accuracy
Number of training pixels		9249	11323	13785	19426	53783
Classification method	Maximum likelihood	9110	11285	12753	18080	95.94%
	FCM	8820	10951	12896	17094	93.42%
	Proposed method	9235	11291	13127	18586	97.62%

TABLE 6: The classification results by proposed algorithm, conventional maximum likelihood and FCM algorithm from IKONOS high resolution satellite image

4) The supervised classification technique using Gabor Filter for the textural attribute to the high resolution satellite image. The author proposed a wavelet transform and Gabor filter based texture analysis for the recognition of water bodies from satellite images including other object on Earth surface [42]. The authors proposed two approaches namely pixel by pixel classification technique approach and object oriented image analysis for classification of water bodies and other land cover in a satellite image [43]. The authors proposed a mathematical morphological analysis approach for detecting water bodies form satellite image. They also suggest chromaticity analysis for removal of atmospheric differences between images [44].

5) The spectral, spatial, and textural features for each region are generated from the thresholded image by dynamic thresholding. Then given these features as attributes, an unsupervised machine learning methodology called conceptual clustering(COBWEB/3) is used to cluster the regions found in the image into N classes—thus, determining the number of classes in the image automatically. This technique is applied successfully to ERS-1 synthetic aperture radar (SAR), Landsat Thematic Mapper (TM), and NOAA advanced very high-resolution radiometer (AVHRR) data of natural scenes. Fig. 11 shows an original SAR sea ice image that consists of packed ice with very dark, cutting linear structures (leads) and grayish regions (new ice or open water). Moreover, there are brighter, silky structures (possibly deformed first year ice) straining within the grayish regions. Therefore, there are essentially four classes in the image.
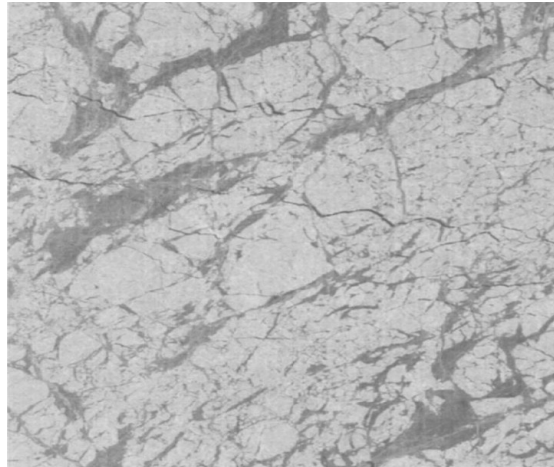
Figure 11: Original ERS-1 SAR sea ice image (March 27, 1992, 73.46 N, 156.19E).ESA

Fig. 12(a) shows the Yellow River plain, Shandong Peninsula, and the delta of Yangtze River at the south in China. It is the infrared band (0.725–1.10 m) of AVHRR, with a resolution of 1500 m/pixel. The image was a composite of a ten-day series, taken during September 1–10, 1992. In the image, the dark regions are bodies of water (sea, rivers, and lakes). To the west of the region lies the mountain range of Taihang. To the south of the region lies the mountain range of Dabie. Fig. 12(b) shows the segmentation results. The class labels are as follows:

1) black—water;
2) bright green—saline meadow;
3) orange—temperate coniferous forest and grassland;
4) dark green—warm temperate crops (rice) and deciduous
coniferous forest;
5) yellow—scrub (mountains);
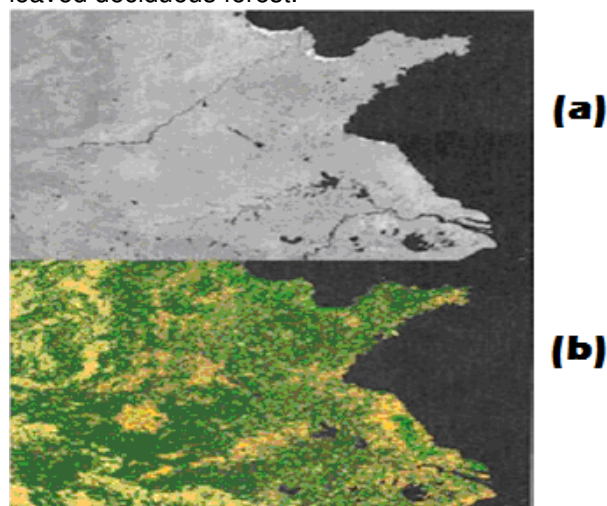6) red—possibly broad-leaved deciduous forest.

Figure 12: (a) Original AVHRR image. (b) The result of our segmentation: six classes

6) The unsupervised classification in 15–30 classes was used for distinguishing between land and water (Fig 13). The 381 AVHRR scenes selected from the cloud algorithm were classified, using all channels. Extending back in time, Landsat data prior to 1985 and for the year 1986 was used for estimating flooding independently for 8 months (November 1972, May–June 1979, May–August 1984, November 1986). The Okavango Delta covers 4 Landsat scenes, and for each of these dates at least 3 Landsat scenes were available. If needed, the data gap (i.e. the 4th quadrant) was filled by dates with similar flooding patterns to the other.

The size discrepancy in total flooded area between the AVHRR estimated floods against ATSR/Landsat estimated floods (columns 2 and 4 in Table 2) varies between 6 and 1351 km^2, averaging at 509 km^2, or 11%. The spatial discrepancy is given as the percentage of the AVHRR derived flooding falling inside the ATSR/Landsat derived flood (column 5 in Table7). This spatial accuracy varies between 63% and 89% (79% – 89% for full scenes).
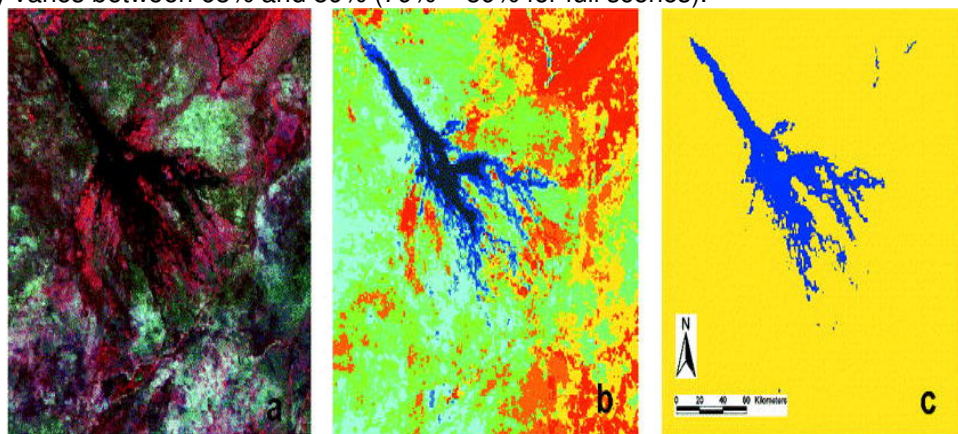

Figure 13: Classification steps a) original AVHRR scene (rgb 1, 2, 3) (date 25 August 1998); b) unsupervised classification in 10 classes; and c) water – land classification

Date	AVHRR(km^2)	Date	Reference Landsat (km^2)	AVHRR correct (%)
5 July 1994	7387	7 Jul/1 Aug 1994	7126	86
4 Dec 1994	(4891)	7 Dec/14 Dec 1994	(4926)	78(only part of image)
15 Feb 1995	(2539)	16 Feb 1995	(3785)	81(only part of image)
7 Oct 1999	6332	10 Oct/2 Nov 1999	6326	84
7 Apr 2000	7936	3 Apr/10 Apr 2000	7958	85
8 Sept 2000	8518	1 Sept/10 Sept/2 Nov 2000	8192	87
			Reference ASTR(km^2)	
25 Aug 1999	7226	30 Aug 1999(8 Sept 1999)	6902	87
3 Sept 1999	7042	2 Sept 1999(8 Sept 1999)	6992	89
19 Sept 1999	6562	18 Sept /21 Sept 1999	5675	79
28 Sept 1999	(6532)	24 Sept 1999	(6304)	85(only part of image)
7 Oct 1999	(5804)	4 Oct 1999	(4706)	73(only part of image)
16 Dec 1999	(5377)	16 Dec 1999	(4026)	63(partly cloudy)

TABLE 7: Accuracy evaluation result derived from cross tabulation of classification and reference data

3.3 Feature Based Classifier
The water-type classification process by applying statistical decision criteria to define class boundaries and assign pixels to a particular class. We have implemented two different feature-based classifiers, the Euclidean Distance Classifier, and the Eigenvector Classifier. The Euclidean Distance Classifier assigns each pixel p_j to a water type i based on the distance between that pixel and the centroid or mean of each class.

3.4 Data Fusion
1) After the feature extraction two change detection methods are applied: a) Image to Image and b) feature based. In image-to-image approach, the multi-temporal images this can be distinguish

between two approaches. An indirect image change detection, where the change analysis follows an image classification process. The comparison can be done by either differencing the two raster classified thematic layers or by extracting the boundaries of the thematic regions and conduct a vector (i.e., feature-based) change analysis. With this approach we overcome problems related to image acquisition conditions, such as different sensors, atmospheric and illumination conditions and viewing geometries. The accuracy of the detected changes is proportional to the accuracy of the image ortho rectification and of the classification results. In the second approach, image rationing, image differencing, image regression and Principal Component Analysis were used. While the feature based approach, the feature-based approach various functions of spatial analysis are used, such as layer union, layer intersection, buffer generation, and topological overlay.

Figure 14: Thresholding on Landsat 7 band 5   **Figure 15**: Extracted water bodies

2) A variety of satellite images of the 1993 flooding in the St. Louis area were evaluated and combined into timely data sets. The resulting maps were valuable for a variety of users to quickly locate both natural and man-made features, accurately and quantitatively determine the extent of the flooding, characterize flood effects and flood dynamics, and easily convey the results to a wide audience. Furthermore, the maps can continue to be used to help track changes over time, characterize the nature of the flooding, identify failures/weak points in the flood control systems, provide input into future flood plain analysis planning, and communicate details about the flooding clean-up work to both the general public and government planners.
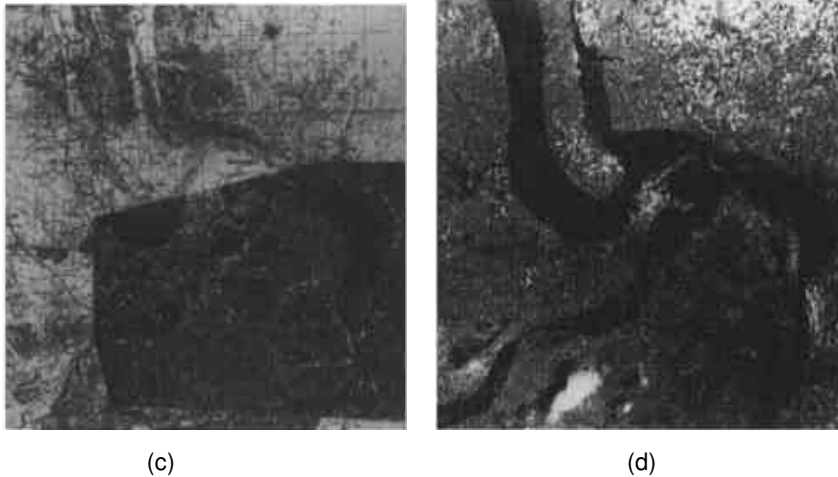

(a)   (b)

(c)   (d)

Figure 16: (a) Reference of normal Mississipsi, Illinois and Missouri River Channel; (b) July 29, 1993 SPOT Image of Flooded areas; (c) July 14, 1993 Satellite Radar Image Superimposed on Reference Map; (d) July 18, 1993 Band 4 Landsat TM Image of Flooded River System using Landsat TM satellite image.
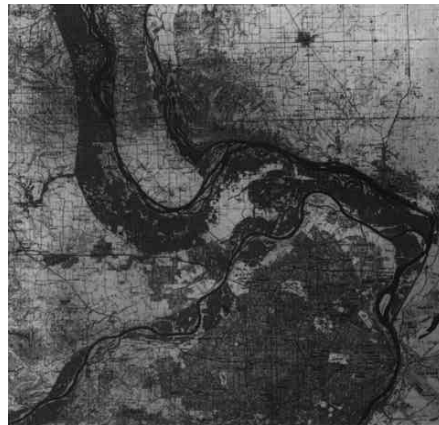

Figure 17: Image Showing Combined Data Sets

The authors proposed an algorithm DRAGON (Drainage Algorithm for Geospatial knowledge) which is a fusion method which is based on image processing and hydrologic modelling. The hydrologic modeling methodology based on modeling stream locations from DTED (Digital Terrain Elevation Data). Satellite imagery provides direct evidence of stream and lake locations, and used to complement and/or supersede stream locations derived from the DTED [45].
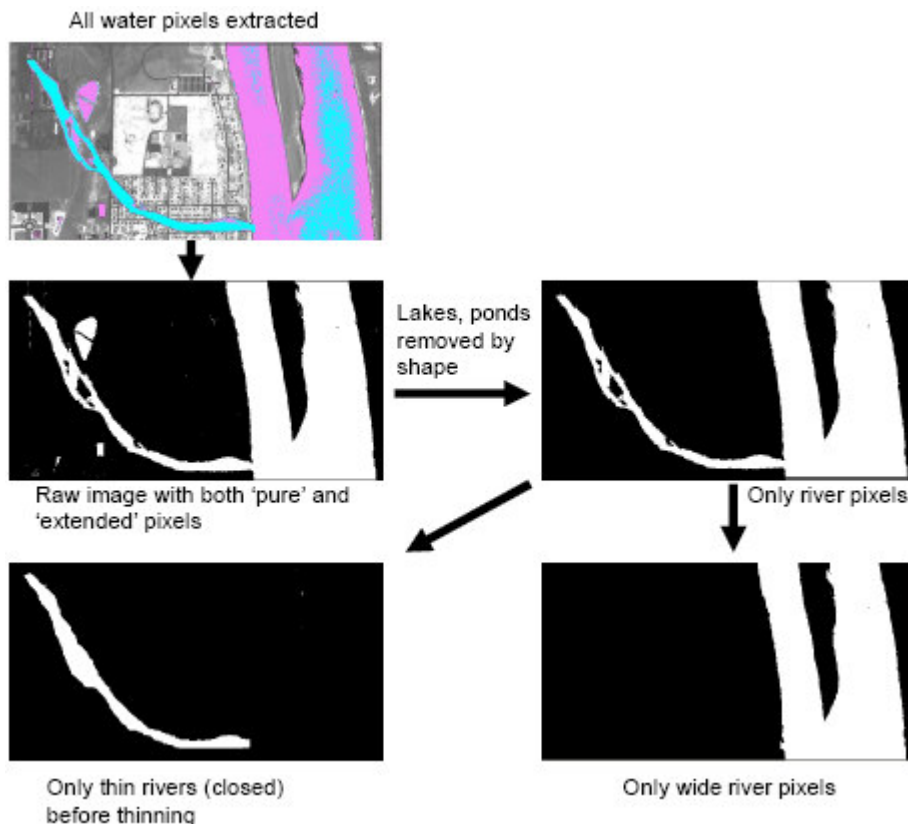
All water pixels extracted

Raw image with both 'pure' and 'extended' pixels

Lakes, ponds removed by shape

Only river pixels

Only thin rivers (closed) before thinning

Only wide river pixels

Figure18: Example of the piecewise refinement used by the DRAGON methodology to extract narrow (< 30m wide) and wide rivers

4. CHALLENGES, CONCLUSIONS, AND THE FUTURE

The distinction of colors between the shadows of tall buildings and calm water surface is still a challenge to the professionals. Therefore, it is difficult to get the exact information about water body in urban areas. To get the exact water in urban areas other similarity checks are required to be performed. Several algorithms were developed for extracting water body but none of them are accepted universally. Hence those are not applicable to various sensor images. Most of them are application specific.

In future the improvement in the water body extraction algorithm is expected, so that the system will be automated for handling all types of sensor images and it will be combined with other tools to provide better information for flood, availability of underground water. These aspects are critical issue in developing countries. Sometimes, it is tedious to collect the ground data manually.

Conclusions: The first part of this paper introduced the importance of water body information, the motivations of performing water feature extraction and the major difficulties in water body segmentation. The paper describes the different types of satellites and sensors used in acquiring satellite images for extracting water feature. Some of the results are discussed. Finally, an attempt has been made to conclude the current challenges as well as the future on water body extraction techniques.

5. REFERENCES

[1]   Noble I. M. Apps, R. Houghton, D. Lashoff, W. Makundi, D. Murdiyarso, B. Murray, W. Sombroek, R. Valentini, R. Lal et al. 2000. Implications of different definitions and generic issues. In: "Land Use, Land Use Change and Forestry". IPCC Special Report, Washington, D.C., 377 pp.

[2]   F. M. Henderson. "Environmental factors and the detection of open surface water areas with X-band radar imagery". International Journal of Remote Sensing, vol. 16(13), pp. 2423 – 2437, September 1995.

[3]   Xie Chunxi , Zhang Jixian , Huang Guoman , Zhao Zheng and Wang Jiaoa. "Water body information extraction from high resolution airborne synthetic aperture radar image with technique of imaging in different directions and object-oriented". In Proceeding of the ISPRS Congress Silk Road for Information from Imagery, Beijing, 2008, pp. 165-168.

[4]   A. Prakash and R. P. Gupta. "Land-use mapping and change detection in a coal mining area - a case study in the Jharia coalfield, India". International Journal of Remote Sensing, vol. 19(3), pp. 391 - 410, Feb 1998.

[5]   Zhang Qiuwen, Wang Cheng, Shinohara Fumio, Yamaoka Tatsuo, "Automatic extraction of water body based on EOS/MODIS remotely sensed imagery". In Proceedings of the SPIE, Volume 6786, pp. 678642, 2007.

[6]   HU Zhuowei , Gong Huili and Zhu Liying. "Fast flooding information extraction in emergency response of flood disaster". ISPRS Workshop on Updating Geo-spatial Databases with Imagery & The 5th ISPRS Workshop on DMGISs, Urumchi, Xingjiang, China, August 28-29, 2007.

[7]   Célia Gouveia and Carlos DaCamara. "Continuous mapping of the Alqueava region of Portugal using satellite imagery". In Proceeding of the EUMETSAT Meteorological Satellite Conference, Helsinki, Finland, 12 - 16 June 2006.

[8]   Costas Armenik and Florin Savopol. "Image processing and GIS tools for feature and change extraction". In Proceeding of the ISPRS Congress Geo-Imagery Bridging Continents, Istanbul, Turkey, July 12-13, 2004, pp. 611-616.

[9]   Cunjian Yang Cunjian Yang Rong He Siyuan Wang. "Extracting water-body from Beijing-1 micro-satellite image based on knowledge discovery". In the Proceeding of the IEEE International Geoscience & Remote Sensing Symposium, Boston, Massachusetts, U.S.A, July 6-11, 2008.

[10]   A Gandhe, V Venkateswarlu and R N Gupta. "Extraction of coal under a surface water body – a Strata Control Investigation". Journal of Rock Mech. Rock Engg vol. 38 (5), pp. 399–410, 2005.

[11]   Patricia G. Foschi, Deepak Kolippakkam, Huan Liu and Amit Mandvikar. "Feature extraction for image mining". In Proceeding of the Multimedia Information Systems Conf., pp. 103-109, 2002.

[12]   Kaichang Di, Ruijin Ma, Jue Wang, Ron Li., "Coastal mapping and change detection using high-resolution IKONOS satellite imagery". In Proceedings of the 2003 annual national conference on Digital government research, Boston, MA, vol.130, pp 1 – 4,2003.

[13] Ojaswa Sharma, Darka Mioc and François Anton. "Feature extraction and simplification from color images based on color image segmentation and skeletonization using the quad-edge data structure". In Proceeding of the 15th International Conference in Central Europe on Computer Graphics, Visualization and Computer Vision'2007.

[14] Kaichang Di, Ruijin Ma, Jue Wang, Ron Li. "Automatic shoreline extraction from high-resolution IKONOS satellite imagery". In Proceedings of the 2003 annual national conference on Digital government research, Boston, MA, vol.130, pp 1 – 4,2003.

[15] Yuanzhi Zhang, Jouni T. Pulliainen, Sampsa S. Koponen, and Martti T. Hallikainen. "Water quality retrievals from combined Landsat TM data and ERS-2 SAR data in the Gulf of Finland". IEEE Transaction on GEOSCIENCE AND REMOTE SENSING, 0196-2892, 2003.

[16] Leen-Kiat Soh and Costas Tsatsoulis. "Segmentation of satellite imagery of natural scenes using data mining". IEEE Transactin On GeoScience and Remote Sensing, vol. 37(2), pp. 1086-1099, 2005.

[17] Zhang Zhaohui, Veronique Prinet and MA Songde. "Water body extraction from multi-source satellite images". IEEE, 0-7803-7929-2/03, 2003.

[18] Jenny M. McCarthy, Thomas Gumbricht, Terence McCarthy, Philip Frost, Konrad Wessels, and Frank Seidel. "Flooding patterns of the Okavango wetland in Botswana between 1972 and 2000". AMBIO: A Journal of the Human Environment, vol. 32(7), pp. 453-457, November, 2003.

[19] Linda V. Martin Traykovski and Heidi M. Sosik. "Optical classification of Northwest Atlantic water types based on satellite ocean color data". Biology Department, MS 32, Woods Hole Oceanographic Institution, Woods Hole, MA 02543.

[20] Gidudu Anthony, Hulley Greg and Marwala Tshilidzi. "Classification of images using support vector machines". arXiv: 0709.3967v1, Cornell University, Library, 2007.

[21] Habibullah U Abbasi, Mushtaq A Baluch and Abdul S Soomro. "Impact assessment on Mancher lake of water scarcity through remote sensing based study". In Proceeding of GIS, Saudi Arabia.

[22] Ana Carolina Nicolosi da Rocha Gracioso, Fábio Fernando da Silva, Ana Cláudia Paris and Renata de Freitas Góes. "Gabor filter applied in supervised classification of remote sensing images". In Symposium Proceeding of the SIBGRAPI 2005.

[23] Young-Joon Jeon, Jae-Gark Choi, and Jin-Il Kim. "A study on supervised classification of remote sensing satellite image by bayesian algorithm using average fuzzy intracluster distance". R. K lette and J. Žunić (Eds.): IWCIA 2004, LNCS 3322, pp. 597–606, 2004.

[24] Alecu Corina, Oancea Simona, and Bryant Emily. "Multi-resolution analysis of MODIS and ASTER satellite data for water classification". In Proceedings of the SPIE, the International Society for Optical Engineering, San Jose CA, ETATS-UNIS 2006.

[25] L.M. Fuller, T.R. Morgan, and S.S. Aichele. "Wetland delineation with IKONOS high-resolution satellite imagery, Fort Custer Training Center, Battle Creek, Michigan, 2005". Scientific Investigations Report 2006–5051.

[26] Jean-Francois Cayula and Peter Cornillon. "Edge detection algorithm for SST algorithm". Journal of Atmospheric and Oceanic Technology, vol. 9, pp 67-80, 1992.

[27] G M Petrie, G.E. Wukelic, C.S. Kimball,K.L. Steinmau and, D.E. Beaver. "Responsiveness of satellite remote sensing and image processing technologies for monitoring and evaluating 1993 Mississippi River flood development using ERS-1 SAR, LANDAST, and SPOT digital data". In Proceeding of the ASPRS/ACSM, Reno, NV, 1994.

[28] Nandish M. Mattikalli and Keith S. Richards. "Estimation of surface water quality changes in response to land use change: application of the export coefficient model using remote sensing and geographical information system". Journal of Environmental Management vol. 48, pp. 263–282, 1996.

[29] O S Mudenda and E Nkonde. "The man-made satellite; an instrument of opportunity". In CD-ROM Proceeding of the WMO Technical Conference on Meteorological and Environmental Instruments and Methods of Observation (TECO-2005) Bucharest, Romania, 4-7 May.

[30] Patrick Brezonik, Kevin D. Menken and Marvin Bauer. "Landsat-based remote sensing of lake water quality characteristics, including chlorophyll and colored dissolved organic matter (CDOM)". Journal of Lake and Reservoir Management 21(4), pp. 373-382, 2005.

[31] Leif G. Olmanson, Steve M. Kloiber Patrick L. Brezonik and Marvin E. Bauer. "Use of satellite imagery for water clarity assessment of Minnesota's 10,000 Lakes". University of Minnesota.

[32] A. G. Dekker, T. J. Malthus, M. M. Wijnen and E. Seyhan. "Remote sensing as a tool for assessing water quality in Loosdrecht lakes". Journal of Hydrobiologia, vol. 233, pp. 137-159, 1992.

[33] Panu Nuangjumnong , Ramphing Simking. "Automatic Extraction of Road and Water Surface from SPOT-5 Pan-Sharpened Image". In Proceeding of the Conference Map Asia, 2009.

[34] Hafeez MM, Chemin Y, Van De Giesen, and Bouman B A M. "Field Evaporation in Central Luzon, Philippines, using different sensors: Landsat 7 ETM+, Terra Modis and Aster". In Proceeding of the Symposium on Geospatial Theory, Processing and Applications, Ottawa, 2002.

[35] Magsud Mehdiyev, Ryuzo Yokoyama and Lal Samarakoon. "DETECTION OF WATER-COVERED AREAS BY USING MODIS IMAGERY". In Proceeding of the GeoInfo Conference, ACRS2004, Chiang Mai, Thailand, October 25-30, 2004.

[36] C. Yang, R. Duraiswami, N. Gumerov and L. Davis. Improved Fast Gauss Transform and Efficient Kernel Density Estimation. In Proceeding of the IEEE International Conference on Computer Vision, pages 464-471, 2003.

[37]   C. Yang, R. Duraiswami, D. DeMenthon and L. Davis. Mean-Shift Analysis Using Quasi-Newton Methods. In Proceeding of the IEEE International Conference on Image Processing, pages 447 - 450, vol.3, 2003.

[38]   Janke, R., R. Murray, J. Uber, R. Bahadur, T. Taxon and W. Samuels, 2007. "Using TEVA to assess impact of model skeletonization on contaminant consequence assessment and sensor placement design". In Proceeding of the World Environmental and Water Resources Congress, Tampa, FL, May 15-19.

[39]   H. Sundar, D. Silver, N. Gagvani, S. Dickinson. "Skeleton Based Shape Matching and Retrieval". In Proceedings of the Shape Modeling International 2003, p.130, May 12-15, 2003.

[40]   Chulhee Lee, David Landgrebe. "Feature Extraction And Classification Algorithms For High Dimensional Data". School of Electrical Engineering Purdue University West Lafayette, Indiana 47907-1285, TR-EE 93-1, January 1993.

[41]   Kefei Wand and Yifeng Zhu. "Recognition of Water Bodies from Remotely Sensed Imagery by Using Neural Network". UNIVERSITY OF NEBRASKA - LINCOLN, CSE873 COMPUTER VISION.

[42]   Mariana Tsaneva, Doyno Petkov. "RECOGNITION OF OBJECTS ON THE EARTH'S SURFACE THROUGH TEXTURE ANALYSIS OF SATELLITE IMAGES". In Proceeding of the Third Scientific Conference with International Participation SPACE, ECOLOGY, NANOTECHNOLOGY, SAFETY 27–29 June 2007, Varna, Bulgaria.

[43]   MARIE-CATHERINE MOUCHOT, THOMAS ALFOLDI, DANIEL DE LISLE and GREG McCULLOUGH. "Monitoring the Water Bodies of the Mackenzie Delta by Remote Sensing Methods". ARCTIC, VOL. 44, SUPP. 1 (1991), PP. 21-28.

[44]   T Van de, W De Genst, F Canters, N Stephens, E Wolf, and M Binard. "Extraction of Land Use/ Land Cover-Related Information from very High Resolution Data in Urban and Suburban areas". In proceeding of the 23rd EARSeL Annual Symposium on June 3, 2003.

[45]   Gregg Petrie, Brain Moon, and Karen Steinmaus. "Semi-automated stream extraction at PNNL". In proceeding of the Overwatch Geospatial Users Conference, 2008.